Self-adaptive Controllers for Renewable Energy Communities Based on Transformer Loading Estimation

Citation for the original published paper (version of record):

N.B. When citing this work, cite the original published paper.

(article starts on next page)

Self-adaptive Controllers for Renewable Energy Communities Based on Transformer Loading Estimation

Minh-Quan Tran, Trung Thai Tran, Phuong H. Nguyen
Department of Electrical Engineering
Eindhoven University of Technology
Eindhoven, The Netherlands
{m.q.tran, t.t.tran, p.nguyen.hong}@tue.nl

Tam T. Mai
DNV Netherlands B.V.
Arnhem, The Netherlands
tam.mai@dnv.com

Le Anh Tuan
Department of Electrical Engineering
Chalmers University of Technology
Gothenburg, Sweden
tuan.le@chalmers.se

Abstract—In this paper, self-adaptive controllers for renewable energy communities based on data-driven approach are proposed to mitigate the voltage rise and transformer congestion at the community level. In the proposed approach, the transformer loading percentage is estimated by the trained data-driven model, which uses the extreme gradient boosting regression algorithm based on a measurement set acquired from critical coupling points of the communities. To avoid voltage rise issues, the droop control parameters (i.e., voltage threshold for $P - V$, $Q - V$ curves) are adaptively tuned based on the solar irradiance availability and estimated transformer loading. The proposed approach has been tested in the IEEE European LV distribution network. Results showed that the control approach could effectively reduce 22.2% of the total overloaded instances, while still keeping voltage magnitude in the operation range. This method can help DSOs manage voltage violation and congestion without further communication.

Index Terms—Droop control, transformer loading estimation, transformer congestion, voltage rise.

I. INTRODUCTION

Power systems are facing challenges while integrating a massive amount of distributed energy resources (DER), especially at the distribution network level due to a lack of advanced monitoring and control solutions [1], [2]. Either voltage violations or overloading of network assets, i.e. transformer, power cables, are observed that hinder the integration of DERs. Proper control coordination of DERs is expected to be an effective solution to avoid large investment for network upgrade and extension.

DER control solutions have been proposed to cope with each of these issues (i.e., voltage rise and transformer congestion) separately. On the one hand, the overvoltage mitigation solutions have been extensively studied [3], [4]. In [3], solutions were proposed for overvoltage mitigation based on droop control, i.e., $P - V$, $Q - V$. To improve the performance of the local droop in terms of fair curtailment, our previous study has shown the advantage of using consensus-based algorithm

to allocate better curtailment resources within specific control areas [4]. Meanwhile, solutions for transformer overloading have been limited to some research works, e.g., by exploring flexibility resources from the demand-side [5]–[7].

There is, however, a strong correlation between voltage violation and overloading of network assets. In [8], the impact of controlling DERs to cope with transformer overloading and overvoltage has been discussed. The authors in [9], [10] addressed the same issues with a solution to coordinate existing controllers including on-load tap changer connecting the medium and low-voltage networks. However, these works are based on an assumption of having perfect information and controllability over DERs and control assets which are not likely the case in reality.

Having awareness of asset loading would be valuable for DERs to not only control voltage at the coupling point, i.e., local impact, but also manage active and reactive power properly. In our previous work, an estimation of transformer loading is developed based on training data with the model-based random tree of a critical set of voltage measurement [11]. In this paper, we proposed a self-adaptive control (SAC) scheme for DER clusters which inherits the sequential droop control (SDC) method while having an awareness of asset (transformer) loading. Overall, the main contributions of this paper are twofold:

- The data-driven transformer loading estimation is adopted to provide the monitoring function to the congestion management, which is trained using extreme gradient boosting regression (XGBR) algorithm. With this monitoring signal, the transformer loading can be controlled in real-time.
- The SAC scheme for renewable communities is proposed that solves the transformer overloading problems, while mitigating voltage rise issues due to high PV penetration in the distribution networks. This proposed control strategy can be adopted by the energy communities to solve the grid issues.

The IEEE European LV distribution network with collected

PV data in the Netherlands is used to test the proposed control. The numerical results showed that the proposed control could effectively reduce the transformer overloading period while mitigating the voltage rise issues.

II. PROBLEM FORMULATION

This section elaborates the transformer overloading issue in the distribution network related to the uses of the SDC method.

A. Sequential Droop Control

The SDC method regulates the power outputs of PV systems based on the local available information to solve the voltage rise problems. This method is formulated by combining $Q-V$ and $P-V$ droop control scheme in a sequential manner. The SDC method is schematically shown in Fig. 1 and mathematically expressed in Eq. 1 and Eq. 2. The $\underline{V} = 0.9$ p.u. and $\overline{V} = 1.1$ p.u. are the lower and upper limits of voltage control. Given house i in the network, V_i^{gQ} and V_i^{tQ} (at point (1)) are the threshold level for reactive power injection and absorption, respectively. V_i^{tP} at point (2) is the threshold level for active power curtailment.

$$
Q_i^{\text{net}} = \begin{cases} \overline{Q}_i \dfrac{(V_i^{gQ} - V_i)}{(V_i^{gQ} - \underline{V})}, & \text{if } \underline{V} \leq V_i < V_i^{gQ} \\ 0, & \text{if } V_i^{gQ} \leq V_i \leq V_i^{tQ} \\ -\overline{Q}_i \dfrac{(V_i - V_i^{tQ})}{(V_i^{tP} - V_i^{tQ})}, & \text{if } V_i^{tQ} < V_i \leq V_i^{tP} \\ -\overline{Q}_i, & \text{if } V_i^{tP} < V_i \leq \overline{V}, \end{cases} \tag{1}
$$

$$
P_i^{\text{net}} = \begin{cases} P_i^{\text{MPP}}, & \text{if } \underline{V} < V_i \leq V_i^{tP} \\ P_i^{\text{MPP}} - P_i^{\text{MPP}} \dfrac{(V_i - V_i^{tP})}{(\overline{V} - V_i^{tP})}, & \text{if } V_i^{tP} < V_i < \overline{V} \\ 0, & \text{if } V_i \geq \overline{V}, \end{cases} \tag{2}
$$

In normal operation, i.e., voltage magnitude at the point of connection (POC) V_i in the range from V_i^{gQ} to V_i^{tQ}, the
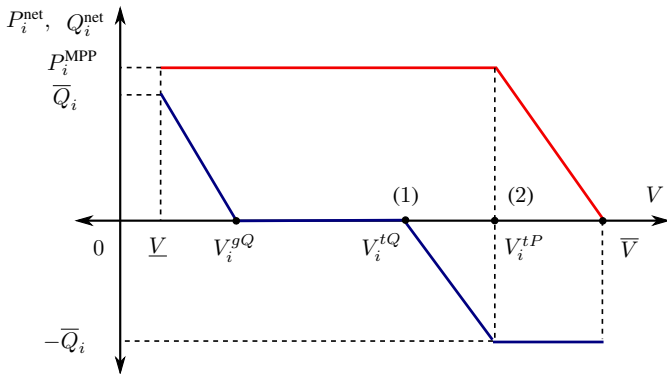

Fig. 1: The SDC mechanism applied for PV unit i connect to bus i, the SDC consists of $Q-V$ droop control (dark blue curve) and $P-V$ droop control (red curve).

reactive power output of PV inverter is set to zero, while the active power injection P_i^{net} is set to P_i^{MPP}, the maximum power point. When V_i exceeds V_i^{tQ}, the PV inverter starts absorbing reactive power following $Q-V$ droop. If V_i is increased higher than V_i^{tP}, then the reactive power absorption is set to maximum value $-\overline{Q}_i$, and the active power output is curtailed follow $P-V$ droop. The $\overline{Q}_i$ is calculated as follows:

$$
\overline{Q}_i = \min(\overline{Q}_{i1}, \overline{Q}_{i2}) \tag{3}
$$

$$
\overline{Q}_{i1} = \sqrt{(S_i)^2 - (P_i^{\text{net}})^2}, \tag{4}
$$

$$
\overline{Q}_{i2} = (\tan[\arccos(\text{PF})]) P_i^{\text{net}}, \tag{5}
$$

with S_i is PV inverter apparent power, P_i^{net} is active power output, and the power factor ranging from 0.9 lagging to 0.9 leading for PV connected at distribution network [12].

B. Transformer Loading

The SDC method is presented in section II-A, which mitigates the voltage rise issue while reducing the amount of active power curtailment. To do so, reactive power absorption is used together with active power curtailment. It can significantly reduce the amount of active power curtailment. An example of a radial feeder with installed PVs is shown in Fig. 2. The apparent power flow through the transformer is calculated as follows:

$$
\begin{aligned} S^{trans} &= \sqrt{(P^{trans})^2 + (Q^{trans})^2} \\ &= \sqrt{\left(\sum_{i=1}^{n}(P_i^{PV} - P_i^{L})\right)^2 + \left(\sum_{i=1}^{n}(Q_i^{PV} + Q_i^{L})\right)^2} \end{aligned} \tag{6}
$$

where, n is a number of buses, for this simple example we assume that every bus has a connected PV and a load. It can be seen from Eq. 6, the apparent power of the transformer is increased due to the active power injection (P_i^{PV}) to/reactive power absorption (Q_i^{PV}) from the external grid. Thus, during the high irradiance condition, the transformer can be overloaded while solving the voltage rise issue. Without having an awareness of the asset loading, the controllers with location-specific focuses might worsen the loading of transformers, leading to the degradation of network assets.

III. PROPOSED CONTROL STRATEGY

The proposed control strategy aims to mitigate voltage rise along the feeder due to high PV generation and solve the overloading of the distribution transformers. In this regard, the regression-based method is first employed to estimate the transformer loading. Next, the SAC method is formulated to solve both voltage rise and transformer overloading issues by coordinating PV systems in the network.

A. Data-driven Transformer Loading Estimation

The data-driven method for transformer loading estimation is adopted from our previous study [11]. This data-driven

method is trained to realize the relationships between the transformer loading and voltage magnitudes measured at the POC. Accordingly, a regression model is obtained to estimate transformer loading from a set of measured voltage magnitude.

The regression model utilizes the XGBR algorithm which is an ensemble tree algorithm with the aim of minimizing the objective function given as [13],

$$\sum_{i=1}^{N} l(y_i, \hat{y}_i^{(t-1)} + f_t(x_i)) + \Omega(f_t) \tag{7}$$

where N is the size of data, $\hat{y}_i^{(t-1)}$ denotes the prediction output at the $(t-1)$-th (i.e., previous) iteration of the i-th instance, y_i denotes the observation, f_t denotes the independent tree structure at the t-th iteration, l denotes the loss function measuring the difference between y_i, $\hat{y}_i^{(t-1)}$, and f_t, and $\Omega(f_t)$ denotes the penalty term for the model complexity. The term $\Omega(f)$ can be calculated as,

$$\Omega(f) = \gamma L + \frac{1}{2}\alpha||\omega^2|| \tag{8}$$

where L is the number of leaves in the tree, ω is the score of leaves, and γ and α are regularisation coefficients [14].
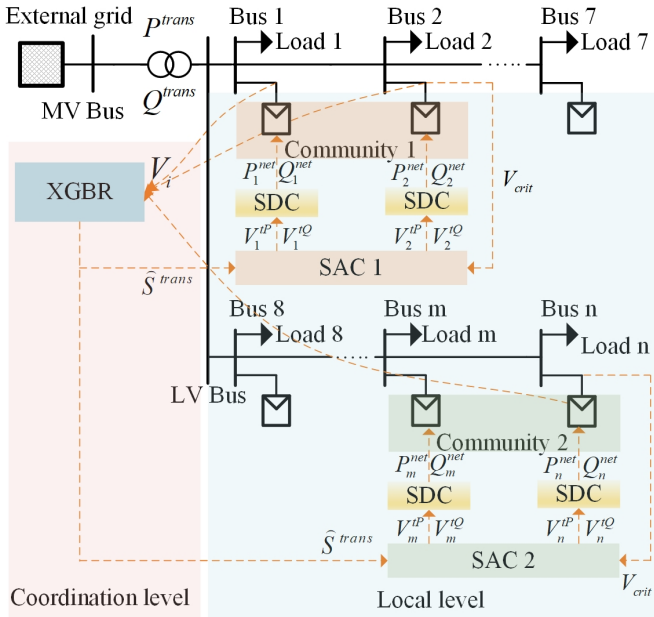

Fig. 2: The proposed control architecture with installed PVs. P^{trans}, Q^{trans} are the active, reactive power flow via the transformer. $\hat{S}^{trans}$ is the estimated apparent power of transformer. V_i^{tP}, V_i^{tQ} are input control signal for SDC. The $(P_i^{\text{net}}, Q_i^{\text{net}})$ are the input control signal of PV inverters. Lastly, V_{crit} is critical voltage of each community.

B. Self-Adaptive Controller

Fig. 2 presents the control architecture of the proposed control method. This strategy consists of two layers: a local control, which is presented in section II-A and a coordination control layer. The local control is based on the SDC mechanism, and the coordination control is based on a regression-based transformer loading estimation mechanism, which is presented in section III-A. The local control layer is responsible for continuously monitoring the voltage at the POC and regulating the active and reactive power of PV units. The coordination control layer, which operates with a lower response speed than the local control layer, is responsible for adequately coordinating PV systems for both the voltage level violations and transformer overloading by periodically adjusting set-points of the local control layer.

As can be seen in Fig. 2, the output power set points of the PV inverters ($P_i^{\text{net}}, Q_i^{\text{net}}$) are determined by the local control layer, which regulates the active power curtailment and reactive power absorption scheme of PV units in response to the voltage at POC follow the droop setting. Furthermore, the $P - V$ and $Q - V$ droop control parameters, i.e., the threshold levels (V_i^{tP} and V_i^{tQ}), are adaptively calculated by the coordination control layer. The coordination control layer is developed as a correction control layer to the local control, which solves the voltage rise issue while preventing the transformer be overloaded.

As discussed in section III-A, the trained XGBR model is able to estimate the transformer loading status with a limited number of voltage measurements from households. Thus, the transformer loading monitoring can be performed within local energy communities. Then, the voltage rise and transformer overloading issues are controlled by communities control architecture, named SAC method. Fig. 3 shows the coordination control algorithm. It is worth noting that the proposed control algorithm is implemented every 15 minutes. The initial value for SDC is started with $V_{i,0}^{tP} = 1.09$ p.u. and $V_{i,0}^{tQ} = 1.05$ p.u., which helps PV inverter inject more active power to the grid. In each community, the node with a higher voltage profile (due to PV active power injection) is selected as critical voltage, V_{crit}, which is located at the end of the feeder. This V_{crit} is used as the input signal for the voltage rise control function. The V_i^{tP} is increased until the critical voltage reaching to 1.09 p.u. The V_i^{tP} is kept constant if the critical voltage is in the band of 1.09 p.u. to 1.1 p.u., this is to prevent the voltage violation due to the control action. When the $V_{crit} \geq 1.1$ p.u., this means the voltage rise happens, the V_i^{tP} is reduced to curtail active power injection from PV inverters (the incremental change of V_i^{tP}, and V_i^{tQ} is $\alpha = \beta = 0.01$, and is chosen by trial and error to minimized voltage violation). Together with voltage rise, the transformer loading status, $\hat{S}^{trans}$, is continuously estimated using the XGBR model. In normal operation, i.e., there is no detected transformer overloading signal, the V_i^{tQ} is reduced to absorb more reactive power. However, when the estimated transformer loading $\hat{S}^{trans}$ exceeds the rated
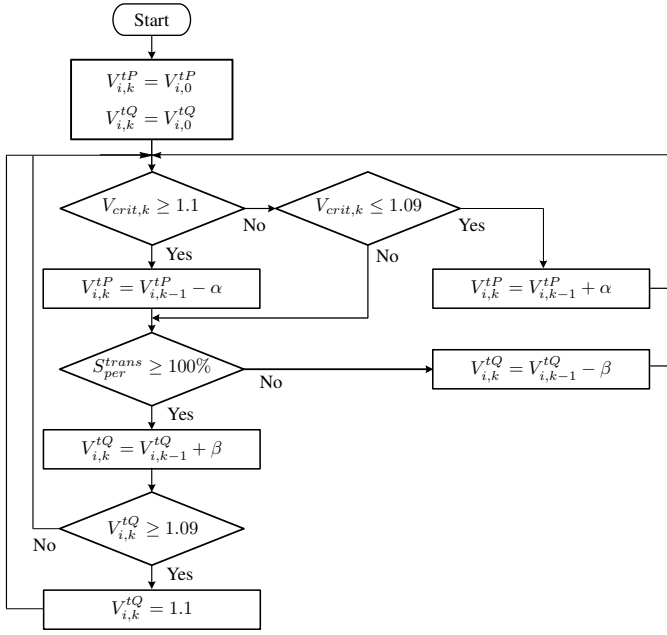
Fig. 3: The flowchart of the SAC algorithm. $V_{i,k}^{tP}$ and $V_{i,k}^{tQ}$ are the threshold value of PV unit i at timestep k. α and β are incremental change of V_i^{tP}, and V_i^{tQ}.
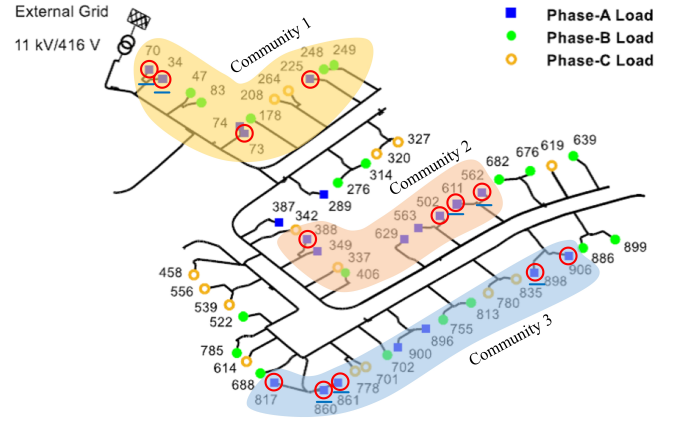

Fig. 4: Single-line diagram of the IEEE European LV test network. It has three different communities which colored with different colors. The houses with a red circle are controllable PV units, seven of them are used as the input for transformer loading estimation (i.e., houses with a blue underline).

power (i.e., $S_{per}^{trans} = \hat{S}^{trans}/S_{rated}^{trans} \geq 100\%$, the voltage threshold for reactive power absorption will be increased to reduce the amount of reactive power absorption. In this sense, the proposed SAC method can adaptively regulate the inputs V_i^{tP}, and V_i^{tQ} for SDC based on the voltage magnitude and transformer loading values.

IV. Test Network and Input Data

This section presents the test network and input data, where the proposed method will be tested. First, the IEEE European 55 buses network is presented. Then, the load profiles, PV systems data are described. Lastly, the training of the XGBR model for transformer loading estimation is explained.

A. LV Test Network

Fig. 4 presents the IEEE European 55 buses network. This is an unbalance three-phase network that is fed by a 250 kVA, 11 kV/0.4 kV distribution transformer [15]. The network has a radial topology supply to its 55 residential users with single-phase connections which consist of 21 houses in Phase A, 19 houses in Phase B, and 15 houses in Phase C. Furthermore, the household is connected with the rooftop PV system. The test network is assumed to have three different local communities, that can access the residential smart meter data and control PV inverter at the customer premises. In this study, the topology of the test network is assumed to remain constant.

B. Load Profiles and PV System Data

Load profiles for the houses in the test network are modeled using real one-year active power data with 15-minute resolution from residential customers' SMs in the Netherlands

[11]. To consider reactive power consumption, all houses are assumed to have a power factor of 0.97 (inductive). The installed PV capacities for this study range randomly from 4.28 kWp to 6.25 kWp, which are based on the actual installations of residential PV in the Netherlands [16]. The PF of ± 0.9 is adopted to model the reactive power capacity of PV units in the test network. Furthermore, for modeling PV generation, the meteorological data, including the solar irradiation data and the ambient temperature are used, which are derived from the real measurements in the Netherlands. As the test network covers a small geographical area, all PV systems are assumed to have the same meteorological data.

V. Training of XGBR-based Regression Model for Transformer Loading Estimation

Proper training of the XGBR-based regression model for transformer loading estimation is vital for performing the proposed control strategy. A procedure is adopted from our previous research [11] to train the XGBR-based regression model for transformer loading estimation. The training procedure is briefly explained into three main stages.

Firstly, an equitable training dataset is prepared, containing stochastic samples of voltage magnitudes and net active and reactive power at the POCs. Such stochastic samples are generated by solving a substantial number of power flows for the test network using the household load profiles and PV system data obtained in section IV-B.

Secondly, exploratory data analysis is implemented on the prepared training dataset, which is followed by the feature selection process. The exploratory data analysis process explores the relationship between the transformer loading and the POC voltage magnitudes. The feature selection aims to select a subset of the most relevant features (the POC voltage magnitudes of which houses) from the dataset for constructing the regression model.
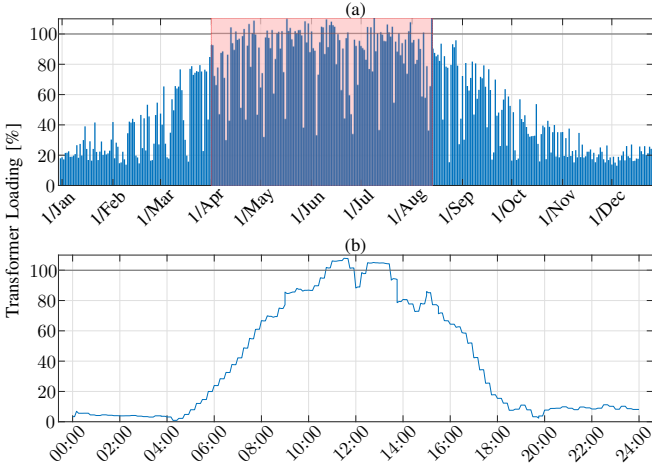
Fig. 5: (a) - One-year transformer loading profile, where PV inverters controlled by SDC method. (b) - One-day transformer loading profile in summer.

Thirdly, given the processed input data, the fitting and evaluation process is performed for the XGBR algorithm, which involves tuning the algorithm parameters and evaluating the generalization error of the model. Nested cross-validation with a $10{\times}10$ set-up for k-fold cross-validation outer loop and inner loop is adopted to carry out this process in an iteration manner.

VI. SIMULATION RESULTS AND DISCUSSION

In this section, the test network, which are described in the previous section will be tested with two control methods, including the SDC, and the proposed SAC method. It should be noted that, only Phase A is used to evaluate the performance of the proposed method. However, without the loss of generality, similar results can be obtained for Phase B and C. As analyzed in our previous work [11], there are 7 important houses (i.e., 70, 34, 611, 562, 860, 898, 861) in Phase A that have a high correlation with the transformer loading status. Having the voltage magnitude of those houses, the transformer loading can be estimated. However, given small-scale residential PV systems, the number of controllable PV is added up to 13 (i.e., the house with the red circle in Fig. 4) to be adequate to solve the transformer overloading issue.

One-year transformer loading profile is shown in Fig. 5(a), where the PV inverters are controlled using the SDC method. It can be seen that the transformer loading is extreme high in the period from mid-April to mid-August, i.e., the colored area in Fig. 5(a). Especially, in some days, the loading is over 100% due to the high active power injection from the PV system. Fig. 5(b) illustrate one-day transformer loading profile in June. It shows the high loading in the mid-day of the transformer. Fig. 6 shows the PDF of transformer loading for the case of using SDC and SAC methods. It can be seen that the proposed method is able to reduce the probability of overloading instances by controlling the PVs power output. In
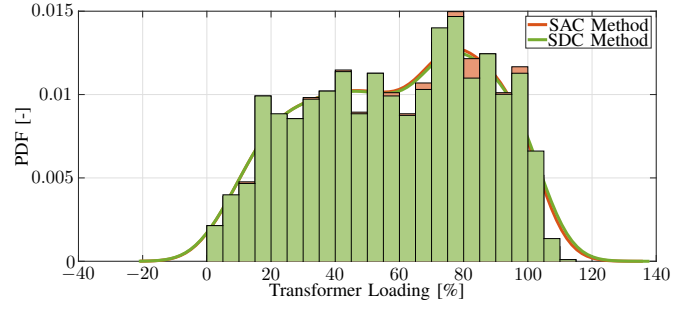

Fig. 6: The probability density function (PDF) of transformer loading for the cases with using SDC and SAC methods.
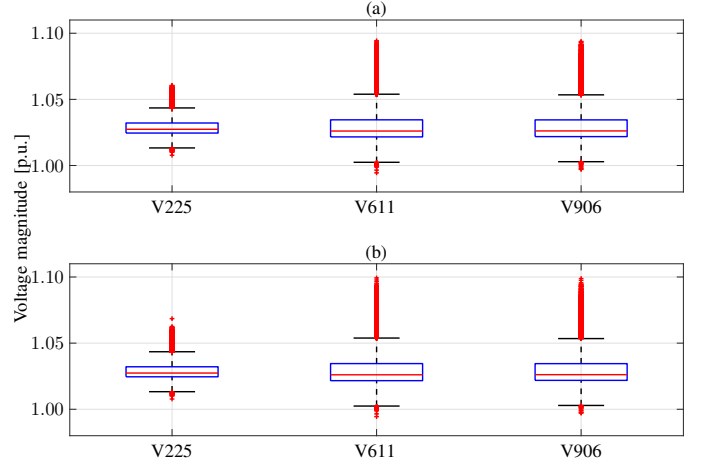

Fig. 7: The box plot of critical voltage magnitude (house 225, 611, and 906 in community 1, 2, and 3, respectively) using SDC (Fig. 7(a)) and SAC (Fig. 7(b)) methods.

addition, the proposed method allow to reduce the amount of active power curtailment in normal operation by increasing the below 100% loading instances of the transformer. The one-year transformer loading profile shows that the proposed SAC method reduced 22.2% of the total overloaded instances (i.e., from 90 to 70) compared to the SDC method. To further evaluate the performance of the proposed method, the box plot of critical voltages in three communities is shown in Fig. 7. As expected, no voltage violations were observed at any time steps when using the SDC method. Similarly, the voltage is controlled by the proposed SAC method. Thus, the proposed SAC method can effectively reduce the period of transformer overloaded and solve the voltage rise issue.

To demonstrate how the proposed method controls the PVs power output, the absolute value of active power injection and reactive power absorption of house 611 is shown in Fig. 8, which corresponds to the transformer loading in Fig. 5(b).It can be seen in Fig. 8(b), the reactive power absorption increases following the increase of active power injection when the loading percentage is still under the limit, i.e., $S_{per}^{trans} < 100\%$. In the case of transformer is being overloaded around 11 AM, i.e., $S_{per}^{trans} \geq 100\%$, the V_i^{tQ} is increased by
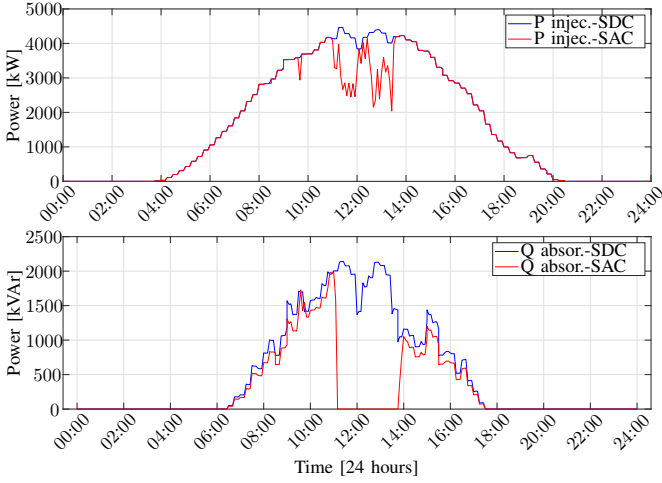
Fig. 8: The active and reactive power profile of house 611 using SAC and SDC methods.

using SAC method to reduce the absorbed reactive power. As a result, the reactive power absorption decreases to zero (i.e., the red curve) to prevent the transformer from overloading. However, the reactive power absorption of PV by using the SDC method (i.e., the blue curve) is kept as the maximum value, $\overline{Q}_i$ in Eq. 3. The transformer overloading issue is still detected even without any reactive power absorption in the SAC method. Thus, the active power injection needs to be curtailed to reduce the transformer loading. The Fig. 8(a) shows that the active power injection in the SAC method (i.e., the red curve) is reduced compared to the active power profile in the SDC method (i.e., the blue curve). This simulation results show the proposed control method can regulate the power output of PVs system to effectively control the voltage rise and transformer overloading issues.

VII. CONCLUSIONS

This paper presents a self-adaptive DER droop controller based on data-driven transformer loading estimation, which solved the voltage rise and transformer overloaded issues. The XGBR technique is employed to estimate transformer loading status with a limited set of voltage magnitudes. Then, the proposed control adaptive calculates threshold values for $P-V$ and $Q-V$ droop controls based on the transformer loading status and voltage magnitude of the critical buses. The simulation results in the IEEE European 55 buses network prove that the proposed method effectively reduces the transformer overloaded period while mitigating the voltage rise issue. By using this control method, the local community can help DSO in managing congestion and voltage violation issues.

As future work, the state estimation method using available customer data can be used to estimate the grid voltage magnitude as well as the transformer overloading. Furthermore, the advantage controller, such as model predictive control also be used to optimize the parameters of the droop controls.

REFERENCES

[1] J. A. Lopes, N. Hatziargyriou, J. Mutale, P. Djapic, and N. Jenkins, "Integrating distributed generation into electric power systems: A review of drivers, challenges and opportunities," *Electric Power Systems Research*, vol. 77, no. 9, pp. 1189–1203, 2007.

[2] R. A. Verzijlbergh, L. J. De Vries, G. P. Dijkema, and P. M. Herder, "Institutional challenges caused by the integration of renewable energy sources in the European electricity sector," *Renewable and Sustainable Energy Reviews*, vol. 75, no. November 2015, pp. 660–667, 2017. [Online]. Available: http://dx.doi.org/10.1016/j.rser.2016.11.039

[3] M. Zeraati, M. E. Hamedani Golshan, and J. M. Guerrero, "Distributed Control of Battery Energy Storage Systems for Voltage Regulation in Distribution Networks with High PV Penetration," *IEEE Transactions on Smart Grid*, vol. 9, no. 4, pp. 3582–3593, 2018.

[4] T. T. Mai, A. N. M. Haque, P. P. Vergara, P. H. Nguyen, and G. Pemen, "Adaptive coordination of sequential droop control for PV inverters to mitigate voltage rise in PV-Rich LV distribution networks," *Electric Power Systems Research*, vol. 192, no. July 2020, p. 106931, 2021.

[5] A. N. Haque, P. H. Nguyen, F. W. Bliek, and J. G. Slootweg, "Demand response for real-time congestion management incorporating dynamic thermal overloading cost," *Sustainable Energy, Grids and Networks*, vol. 10, pp. 65–74, 2017.

[6] I. Bouloumpasis, N. Mirzaei Alavijeh, D. Steen, and A. T. Le, "Local flexibility market framework for grid support services to distribution networks," *Electrical Engineering*, no. 0123456789, 2021. [Online]. Available: https://doi.org/10.1007/s00202-021-01248-y

[7] Z. M. Haider, K. K. Mehmood, S. U. Khan, M. O. Khan, A. Wadood, and S. B. Rhee, "Optimal Management of a Distribution Feeder during Contingency and Overload Conditions by Harnessing the Flexibility of Smart Loads," *IEEE Access*, vol. 9, pp. 40 124–40 139, 2021.

[8] A. N. Haque, P. H. Nguyen, T. H. Vo, and F. W. Bliek, "Agent-based unified approach for thermal and voltage constraint management in LV distribution network," *Electric Power Systems Research*, vol. 143, pp. 462–473, 2017.

[9] J. Quirós-Tortós, L. F. Ochoa, S. W. Alnaser, and T. Butler, "Control of EV Charging Points for Thermal and Voltage Management of LV Networks," *IEEE Transactions on Power Systems*, vol. 31, no. 4, pp. 3028–3039, 2016.

[10] M. Z. Liu, A. T. Procopiou, K. Petrou, L. F. Ochoa, T. Langstaff, J. Harding, and J. Theunissen, "On the Fairness of PV Curtailment Schemes in Residential Distribution Networks," *IEEE Transactions on Smart Grid*, vol. 11, no. 5, pp. 4502–4512, 2020.

[11] T. T. Mai, P. H. Nguyen, N. A. N. M. Haque, and G. A. J. M. Pemen, "Exploring regression models to enable monitoring capability of local energy communities for self-management in low-voltage distribution networks," *IET Smart Grid*, vol. 5, no. 1, pp. 1–17, 2021.

[12] European Committee for Standards - Electrical, "EN 50438:2013 - Requirements for micro-generating plants to be connected in parallel with public low-voltage distribution networks," 2013.

[13] T. Chen; and Carlos Guestrin, "XGBoost: A Scalable Tree Boosting System," *22nd ACM SIGKDD International Conference on Knowledge Discovery and Data Mining*, vol. 19, no. 6, pp. 785–794, 2016.

[14] H. Lu, F. Cheng, X. Ma, and G. Hu, "Short-term prediction of building energy consumption employing an improved extreme gradient boosting model: A case study of an intake tower," *Energy*, vol. 203, p. 117756, 2020.

[15] K. P. Schneider, B. A. Mather, B. C. Pal, C. W. Ten, G. J. Shirek, H. Zhu, J. C. Fuller, J. L. Pereira, L. F. Ochoa, L. R. De Araujo, R. C. Dugan, S. Matthias, S. Paudyal, T. E. McDermott, and W. Kersting, "Analytic Considerations and Design Basis for the IEEE Distribution Test Feeders," *IEEE Transactions on Power Systems*, vol. 33, no. 3, pp. 3181–3188, 2018.

[16] P. P. Vergara, M. Salazar, T. T. Mai, P. H. Nguyen, and H. Slootweg, "A comprehensive assessment of PV inverters operating with droop control for overvoltage mitigation in LV distribution networks," *Renewable Energy*, vol. 159, pp. 172–183, 2020.